Hannula, Jari Matti; Saarinen, Tapio; Holopainen, Jari; Viikari, Ville

Frequency Reconfigurable Multiband Handset Antenna Based on a Multichannel Transceiver

Published in:
IEEE Transactions on Antennas and Propagation

DOI:
10.1109/TAP.2017.2725384

Published: 01/09/2017

Document Version
Peer reviewed version

Please cite the original version:
Hannula, J. M., Saarinen, T., Holopainen, J., & Viikari, V. (2017). Frequency Reconfigurable Multiband Handset Antenna Based on a Multichannel Transceiver. *IEEE Transactions on Antennas and Propagation*, *65*(9), 4452-4460. https://doi.org/10.1109/TAP.2017.2725384

Frequency Reconfigurable Multiband Handset Antenna Based on a Multi-Channel Transceiver

Jari-Matti Hannula, *Student Member, IEEE*, Tapio Saarinen, Jari Holopainen, and Ville Viikari, *Senior Member, IEEE*

***Abstract*—The upcoming standards of wireless communications result in additional and more stringent requirements for antennas in mobile phones. In this paper, we present a frequency-reconfigurable antenna that could potentially be suited for future mobile devices. Frequency reconfigurability is achieved through a cluster of mutually coupled antenna elements that are excited with frequency-dependent weights using a multi-channel transceiver. We report a mobile handset antenna cluster measuring 15 x 15 x 1.6 mm^3 that covers the frequency bands of 1.7–2.7, 3.3–4.5, and 5.475–6.425 GHz with an antenna efficiency better than 90 %. The operation of the antenna cluster is experimentally verified by feeding all the antenna elements with proper weights using tailor-made power splitters that represent a multi-channel transceiver with adjustable amplitude and phase in each branch. The results obtained with the feed networks suggest the feasibility of the reconfigurability concept, and pave way for co-design of the antenna and the transceiver.**

***Index Terms*—Antenna feeds, microwave circuits, mobile antennas, multifrequency antennas**

I. Introduction

WIRELESS communications have significantly improved during the past decades. With the upcoming fifth generation of mobile communications (5G), the capabilities of wireless networks are expected to increase even further. This is required, as the usage of mobile data has been steadily increasing each year and is expected to increase even further. The capacity of 5G networks is projected to increase 1000 times that of the currently used fourth generation (4G) networks to support the increase in wireless traffic [1], [2]. It is generally thought that this increase in capacity could be obtained using a combination of three different approaches: increased spectrum availability, multiple-input multiple-output (MIMO) techniques, and base station densification [3].

In wireless communications, the antenna is a critical component. It is responsible for transmitting and receiving the electromagnetic waves used in the communications. Of the three aforementioned approaches, two apply directly to antenna design. If more spectrum is available for the communications, the antenna should also be able to cover that spectrum. However, for taking advantage of MIMO, several antennas need to be installed in a device. This further limits the available volume for each antenna and causes additional challenges in the form of mutual coupling and correlation between the antennas.

Traditionally, the device would only transmit or receive on one channel. However, with 5G and later releases of 4G, the use of Carrier Aggregation (CA) has been proposed. In CA, the device can transmit or receive on several channels simultaneously for increased data rate. The used channels can exist within the same frequency band (intra-band CA) or in separate bands (inter-band CA). This makes frequency tuning more challenging, as the antenna would have to be tuned to several frequencies at the same time.

It is well known that the electrical size of an antenna has an effect on the obtainable bandwidth and efficiency [4]–[6]. On a mobile device, the space available for an antenna can be very small, making it very difficult to efficiently cover all the required frequency bands. One approach to solving these limitations is frequency tunability. This can be done in mobile communications because the frequency bands used are divided into various channels. Instead of covering all the channels simultaneously, the antenna can be tuned to a specific channel, thus relaxing the bandwidth requirements of the antenna. Approaches for antenna tuning include tunable matching components [7]–[9], switching between multiple matching circuit networks [10] or using, e.g., p-i-n diodes [11], [12] or FET switches [13] to modify the currents in the antenna. The last option is also known as aperture tuning. The problem with these existing tuning methods is that the tuning is relatively narrowband or the tuning network is very lossy. These methods are also not usable with CA because they do not enable independently tunable, simultaneous bands. Alternative methods would therefore be needed.

We presented a theoretical study of a novel approach for obtaining frequency tunability in [14]. Frequency reconfigurability is obtained through a cluster of mutually coupled antenna elements that are excited with frequency-specific weights using a multi-channel transceiver. The study was performed on a monopole antenna array and it showed very promising results. Although this approach has shown great promise for frequency reconfigurability, it has not yet been experimentally verified nor demonstrated with a mobile phone compliant antenna. Other published studies related to this topic include a patent on tunable multi-feed antennas [15] and several studies on eigenefficies of antenna arrays [16]–[18], which we have used to formulate our theory.

In this paper, we apply the aforementioned concept to a

Manuscript received Jan. 13, 2017; revised Apr. 20, 2017 and Jun. 29, 2017; accepted Jul. 3, 2017. Date of publication Month NN, 2017; date of current version Month NN, 2017. This work was supported by Huawei Technologies. The work of J.-M. Hannula was supported in part by Nokia Foundation, Emil Aaltonen Foundation, and Finnish Foundation for Technology Promotion.

The authors are with the Department of Electronics and Nanoengineering, Aalto University School of Electrical Engineering, P.O. Box 15500, FI-00076 AALTO, Espoo, Finland (e-mail: jari-matti.hannula@aalto.fi).

Color versions of one or more of the figures in this paper are available online at http://ieeexplore.ieee.org.

Digital Object Identifier 10.1109/TAP.2017.NNNNNNN

mobile antenna design for studying the feasibility of this concept for future wireless communications. Unlike in [14], we also measure the relevant antenna parameters to validate the operation of our simulated antenna design and to prove the feasibility of this approach to frequency tuning. The full implementation of the concept would require further development in an integrated circuit (IC) transmitter or receiver. Therefore we design two fixed RF phase and amplitude splitter networks to demonstrate how the operating frequency of the antenna can be changed by altering the excitation signal. While they do not fully replicate the behavior of a tunable integrated transmitter, they enable us to demonstrate the frequency reconfigurability of the antenna. Further integrated circuit design is needed to fully realize the concept.

II. Background

A. Specifications

The purpose of this research was to design an antenna for the upcoming fifth generation of wireless communications. While the specifications of 5G are yet to be determined, we can assume the antenna to be required to operate within several frequency bands, including those already used in the existing communications systems. Some spectrum from the C-band has already been allocated to mobile broadband in the World Radiocommunication Conference [19], and there could possibly be further allocations in the sub-6 GHz frequencies. For this study, we have therefore selected the frequency bands to be 1.7–2.7, 3.3–4.5, and 5.475–6.425 GHz.

The focus is on the fast data rate transmissions in an urban environment, so the traditional low band below 1 GHz is not included in this study. Of course, a typical handset should also include the low band. However, including the low band would inherently affect the antenna design, due to the larger size required for the antenna. In addition to covering the low band, there is also the trend of including multiple antennas in the device, to take advantage of the high data rates enabled by, e.g., 8 × 8 MIMO in the 3.5 GHz band. There are several examples of high order MIMO implemented at the higher frequency LTE bands [20]–[23]. These antennas are of course unable to cover the low band due to their small size. As such, there are two different, and in many cases opposite, design goals for mobile antennas.

At this point of the research, the antenna proposed in this paper is somewhat of a compromise between the two cases, with two rather clear future design directions. First, how to make the antenna cover also the low band, and secondly, how to efficiently cover the higher frequency bands with minimal antenna footprint. Thus, the eventual design goal could be a device with main/diversity antennas covering the low band, and several data antennas with the low band excluded. This design strategy would be similar to the one presented in [23].

In this work, the size of the device is in the order of 136 x 68 x 6 mm^3, which is similar to that of current smartphones. The antenna should be fitted within this volume and the antenna element itself should fit to a volume of 15 x 15 x 6 mm^3. For efficient performance, a reflection coefficient < -10 dB is set as the design goal in the operating bands.

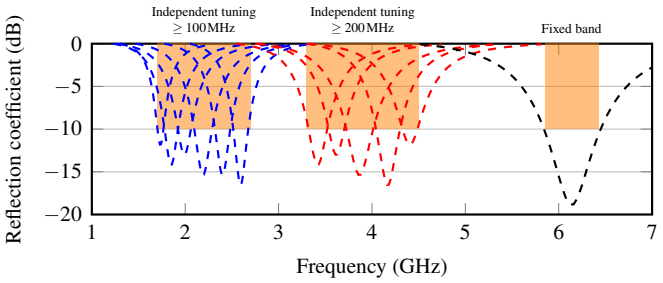

Fig. 1. The specifications of the antenna, showing the three frequency bands and the required instantaneous bandwidths in each band. The bands should be tunable independent of each other.

Additionally, carrier aggregation is to be supported in both inter- and intra-band. This requires the antenna to be independently tunable in the different frequency bands. Fig. 1 shows these specifications. Independent tunability is rather difficult to achieve. Previously shown solutions do not provide this kind of performance. Therefore we design the antenna using the theory derived in [14]. In this approach the antenna cluster is fed using multiple differently weighted feed ports. This approach is explained further in Section II-B.

B. Principle of Operation

In [14] we presented a concept for obtaining frequency reconfigurable operation by creating an antenna system consisting of several closely spaced antennas that are fed simultaneously. By combining the antennas in a varying manner, the operation of the antenna cluster can be changed. Based on the initial investigations performed in the paper, the concept seemed to result in a very wideband tuning range. Thus, we feel that this approach is a suitable candidate for fulfilling the requirements for the antenna.

The concept necessitates that the scattering parameters of the multiport antenna are known. The N-port antenna can then be represented by a scattering matrix

$$\mathbf{b} = \begin{bmatrix} b_1 \\ \vdots \\ b_N \end{bmatrix} = \begin{bmatrix} S_{11} & \cdots & S_{1N} \\ \vdots & \ddots & \vdots \\ S_{N1} & \cdots & S_{NN} \end{bmatrix} \begin{bmatrix} a_1 \\ \vdots \\ a_N \end{bmatrix} = \mathbf{Sa} \qquad (1)$$

where $\mathbf{a}$ is the incident wave vector, $\mathbf{b}$ the reflected wave vector, and S_{ij} the scattering parameters of the antenna system. The antennas are closely spaced and mutually coupled, so the scattering matrix has strong factors in majority of its elements. Because the operation of antennas is frequency dependent, the scattering matrix varies with frequency.

When the system is fed from multiple ports, the individual scattering parameters cannot be used to evaluate the reflection coefficient. The reflection coefficient for each port can be easily calculated from (1) when the system is fed with excitation $\mathbf{a}$ from multiple ports, as the ratio of backward and forward signals in the port. The reflection coefficient is

$$\Gamma_i = \frac{b_i}{a_i} = \frac{1}{a_i}\left(S_{i1}a_1 + S_{i2}a_2 + \ldots + S_{iN}a_N\right). \qquad (2)$$

Thus by weighting the excitations a_i, the reflection coefficient at each port can be modified.

However, instead of looking at each port separately, it is better to evaluate the performance of the entire antenna system. To do so, the Total Active Reflection Coefficient (TARC) can be defined as the square root of the ratio of the total reflected and incident power [24]

$$\mathrm{TARC} = \sqrt{\frac{\mathbf{b}^{\mathrm{H}}\mathbf{b}}{\mathbf{a}^{\mathrm{H}}\mathbf{a}}} = \sqrt{\frac{\mathbf{a}^{\mathrm{H}}\left(\mathbf{S}^{\mathrm{H}}\mathbf{S}\right)\mathbf{a}}{\mathbf{a}^{\mathrm{H}}\mathbf{a}}} \tag{3}$$

where $\mathbf{S}$ is the scattering matrix and $(\cdot)^{\mathrm{H}}$ is the conjugate transpose. Similar to the individual reflection coefficients, the TARC depends on the relative phases and amplitudes of the excitations.

The antenna performance can also be evaluated by accepted power. Instead of TARC, we can thus characterize the performance using matching efficiency

$$\eta_{\mathrm{match}} = 1 - \mathrm{TARC}^2 \tag{4}$$

or as a function of the excitations and the scattering matrix

$$\eta_{\mathrm{match}} = \frac{\mathbf{a}^{\mathrm{H}}\left(\mathbf{I} - \mathbf{S}^{\mathrm{H}}\mathbf{S}\right)\mathbf{a}}{\mathbf{a}^{\mathrm{H}}\mathbf{a}} \tag{5}$$

where $\mathbf{I}$ is the identity matrix. The form of the above equation is a Rayleigh quotient

$$\frac{\mathbf{x}^{\mathrm{H}}\mathbf{M}\mathbf{x}}{\mathbf{x}^{\mathrm{H}}\mathbf{x}} \tag{6}$$

whose largest value is equal to the largest eigenvalue of $\mathbf{M}$, assuming $\mathbf{M}$ is hermitian. This value is obtained when $\mathbf{x}$ is the eigenvector corresponding to that eigenvalue [16]. Therefore the maximum obtainable matching efficiency for an antenna cluster with scattering parameters $\mathbf{S}$ is

$$\eta_{\mathrm{match}} = \max\left\{\mathrm{eig}\left(\mathbf{I} - \mathbf{S}^{\mathrm{H}}\mathbf{S}\right)\right\}. \tag{7}$$

Obtaining this efficiency requires that the system is properly excited. The optimal excitations a_i can be directly obtained from calculating the eigenvalues of $\mathbf{I} - \mathbf{S}^{\mathrm{H}}\mathbf{S}$, and finding the corresponding eigenvector. This complex eigenvector gives directly the amplitude and phase required for the optimal excitation of the antenna.

Matching efficiency is a good figure of merit for the reflected power. However, it does not consider whether the power is radiated or dissipated in the antenna structure. To ensure the power is not lost in the antenna structure due to losses, we also evaluate the total efficiency of the antenna from the far field for the each port separately, and then mathematically combine the radiation patterns to find the total efficiency that is obtainable with the weighted multiport excitation.

Although we use terminology related to transmission here, same principles apply to reception. Instead of weighting the excitations generated by the device, the task is to weigh the incoming signal in the receiver. Due to reciprocity, the antenna performance is the same in both cases. The differences will occur in the transceiver, as the operation of the transmitter and the receiver are different, e.g., in amplifier design (power amplifier or low-noise amplifier), and in the figure of merit: Transmission requires good efficiency whereas reception requires good signal-to-noise ratio.

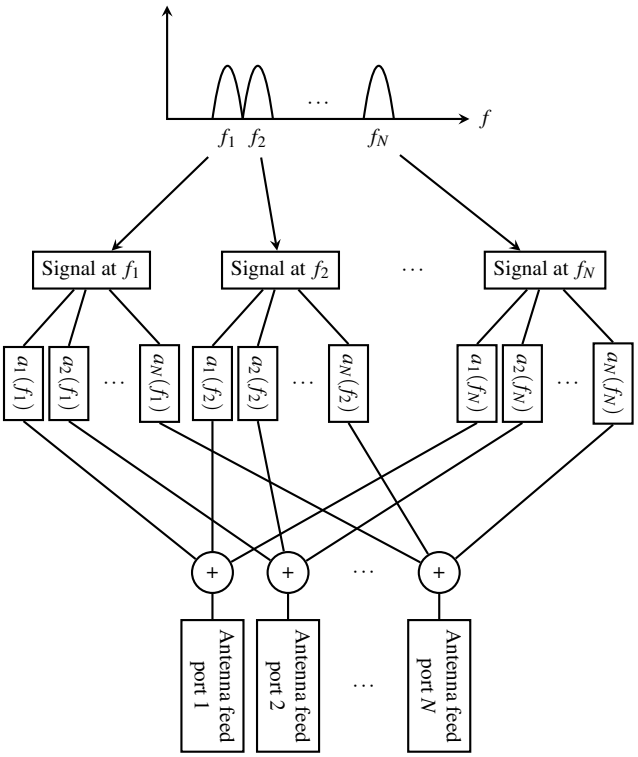

Fig. 2. Multiband operation can be achieved by weighting each component carrier separately, summing differently weighted components together and finally feeding the signals into different antenna feed ports.

C. Multiband Operation

The specifications state that the antenna should be able to operate simultaneously across three frequency bands and each frequency band should be able to be tuned separately. In this section, we explain how this operation can be obtained using our method.

The frequency bands reserved for cellular systems are relatively broad and diverse. Nevertheless, the mobile device has traditionally used only one relatively narrow band at a time. This property has enabled tunable antennas capable of covering one narrow frequency range at a time. However, some new paradigms, such as carrier aggregation use multiple bands simultaneously to increase the bandwidth and thus also the channel throughput. The simultaneous frequencies used by the CA can be in the same or different bands. Traditional reconfigurable antenna tuning solutions cannot be used because they can enable operation only at one frequency at a time. We expect the antenna solution presented in this paper and in [14] to not pose this limitation.

In principle, the multiband operation is achieved by splitting the transmitted (or received) signal into distinct frequency components. These frequency components are then treated as point frequencies and weighted separately such that matching is achieved at every frequency. The differently weighted frequency components are finally combined together and fed to antenna feed ports. The aforementioned procedure can be realized fully digitally or analogically or exploiting partly both. This is analogous to beam steering of an antenna array. The beam steering can be realized in digital domain or RF vector

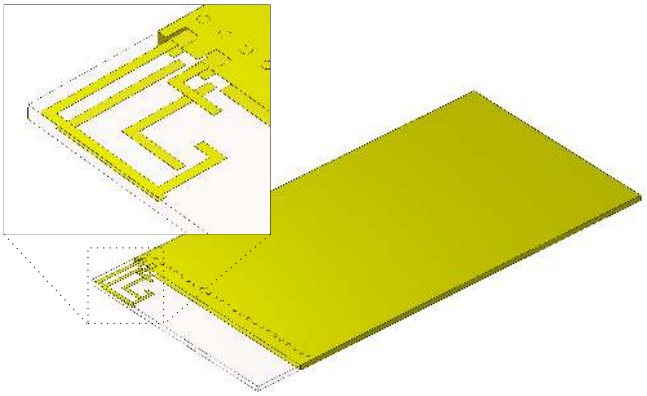

(a)

(b)

Fig. 3. The proposed antenna. (a) Simulated design, (b) Manufactured prototype. The antenna elements are placed on both sides of the substrate.

modulators can be used to manipulate the element weights. Fig. 2 illustrates the principle of the multiband operation. Each component carrier is weighted separately and the differently weighted carrier components are summed together and fed to antenna feed ports.

In this section we have detailed the multiband operation from the antenna point of view. The complete implementation of this depends on the transceiver design. Details on the transceiver implementation are beyond the scope of this paper.

III. Antenna Prototype

A. Antenna Design

We design the antenna on a substrate with a standard thickness of 1.575 mm. The substrate has a dielectric permittivity of $\varepsilon_{\mathrm{r}} = 2.33$ and a loss tangent of $\tan\delta = 0.0012$. There is 15 mm of clearance in the ground plane for the antenna, at the end of the long edge of the ground plane. The dimensions and the overall design of the entire structure are shown in Fig. 3(a).

Instead of considering any individual scattering parameter, the design goal is to maximize (7) across the design frequencies. The number of different variables contributing to (7) makes finding fundamental design rules challenging (10 different scattering parameters for a reciprocal 4-port). Thus, the antenna cluster design is rather experimental at this stage of the research. Nevertheless, some rules can be found.

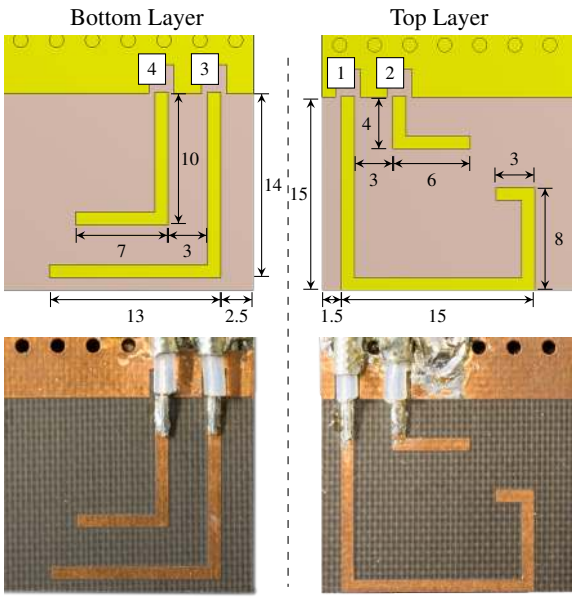

Fig. 4. Close-up of the proposed antenna elements. All dimensions are in millimeters. The width of the antenna elements is 1 mm.

To begin the design process for an antenna using the proposed approach, one should start with the minimum operating frequency of the antenna. This minimum frequency should be adequately covered by one of the elements. This is element numbered 1 as depicted by Fig. 4. To limit the volume taken by the antenna, it is folded several times. This will somewhat reduce the radiation resistance of the antenna and deteriorate the matching. To extend the bandwidth of the antenna system, a second element with slightly higher resonant frequency is placed within the volume defined by the largest antenna element. Because the two elements have close resonant frequencies, they couple power to each other. This coupling can then be used to cancel the reflected waves in both ports, thus reducing the total reflected power.

The design process is then continued by placing smaller elements within the volume defined by the largest element. A good initial guess for their resonant frequencies is to find a frequency where the cluster performance begins to deteriorate, and then extend the bandwidth with the new element. Once all elements are in place, the lengths of the elements are then adjusted to fine-tune the resonant frequencies. The feed placement and the location of the 90-degree turn in the elements is used to further tune the system by adjusting the coupling, which should not be too large as not to destroy the performance nor too small to prevent the reflection cancellation. In addition to the magnitude of the coupling, the phase of the coupling coefficient is also important. Earlier investigations on the antenna cluster concept can be found in [14], [25].

The dimensions of the proposed antenna are shown in Fig. 4 and the corresponding simulated scattering parameters are shown in Fig. 5. TARC is calculated from the scattering parameters using (7). The corresponding eigenvectors for the calculated TARC are depicted in Fig. 6. The amplitude values are normalized in a way that the total power fed from the

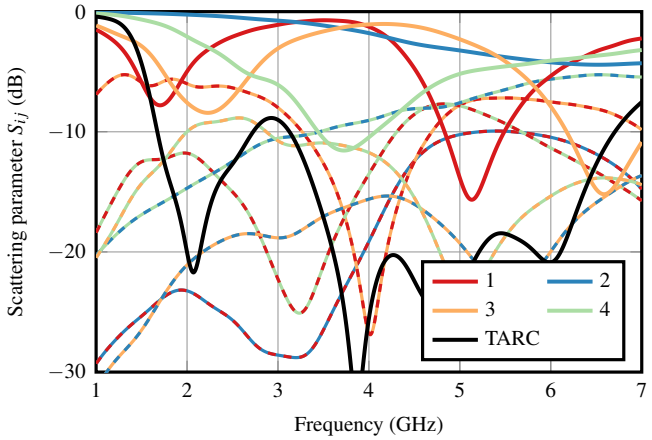

Fig. 5. The magnitudes of the scattering parameters and the corresponding TARC.

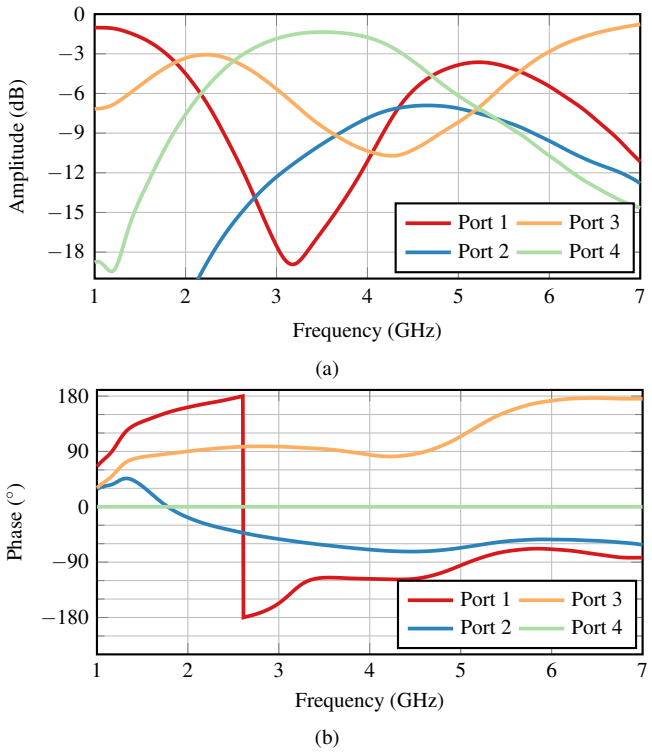

Fig. 6. The (a) amplitude and (b) phase for optimal feeding of the antenna.

ports equals 0 dB. The absolute values of the phases can be arbitrary, as long as the phase differences between the ports remain the same. In this figure the phase of the fourth port has been set as the reference.

Elements 1 and 3 are used to cover the lowest operating band, and their multiresonant behavior produces resonances also around the high band. Element 4 is used to mainly cover the band between the resonances of the first two elements. Finally, element 2 is added to further tune the behavior of the antenna cluster to better cover the desired frequency bands.

Fig. 5 illustrates the strength of the concept. Looking at, e.g., the lowest frequency band, the scattering parameters S_{11} and S_{33} are above -8 dB, and the coupling between those ports is in the order of -6 dB. Yet the total reflected power in the cluster is in the order of -10 to -20 dB, illustrating how the antenna elements work in unison to improve performance.

Fig. 6(a) shows that not all ports need to be able to output the same maximum power. This is something to consider in the amplifier design, e.g., some of the antennas could be driven with smaller amplifiers, which could help with the reduction in efficiency due to operating the amplifier with a lower output power [26]. For example, in this design the second antenna is more of a supporting element, as it is not fed the largest signal at any frequency. Once the limitations of the transceiver with this concept are better known, they are expected to impose limitations and requirements on the antenna design.

Related to the complexity of the transceiver, in our earlier work [14], [25] and also in this paper, the number of antenna elements has been four. Four antenna elements result in increased degrees of freedom in the optimization of the excitation, and thus enable the antenna cluster to operate across a very wide frequency band. This of course results in increased transceiver complexity. Further antenna design could reduce the number of required antenna elements. This could also be done by targeting narrower frequency bands, as opposed to the more continuous tuning targeted in this phase of the research.

The design does not fully use the available 6 mm in the vertical direction. For ease of fabrication, we did not consider three-dimensional antenna structures, but instead only planar antenna geometries printed directly on the substrate. We take some advantage of the vertical space available by placing the antennas on two different layers but further designs should utilize the volume more effectively. By extending the antenna to the third dimension, the footprint of the antenna, and therefore the clearance required, could be reduced. The benefits of three-dimensional antenna elements is something to be investigated in future studies. The antennas could be designed somewhat similarly as in [27], where the antenna is wrapped around a block of substrate.

The proposed antenna has been designed for operation in free space. When designing handset antennas, it is important to also consider the user effect. The question here is that how does the method work in the presence of the user, when the hand or head of the user is in the near field of the antennas. This is something that must be investigated in the future.

B. Manufactured Prototype

We manufactured a prototype based on our simulated design. The prototype is manufactured on a TLY-3 substrate by Taconic. Initially, the feeding was intended to be done with microcoaxial connectors, but the cables introduced losses and uncertainty to the measurements. The feeding was therefore implemented with semi-rigid coaxial cables that were soldered directly to the antennas. The manufactured prototype is depicted in Figs. 3(b) and 4.

IV. Experiments

A. Scattering Parameters and Efficiency

We characterize the prototype by measuring the typical single-excitation parameters, such as the 4-port scattering

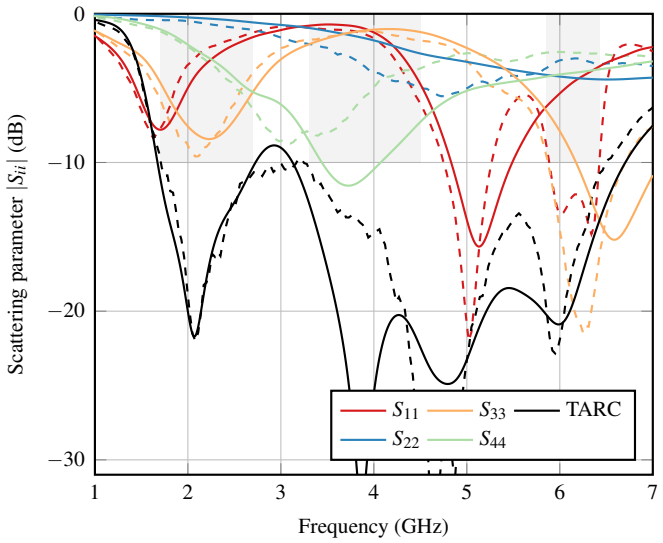

Fig. 7. Measured (dashed lines) and simulated (solid lines) reflection coefficients $|S_{ii}|$ and Total Active Reflection Coefficient (TARC). The TARC fulfills the specifications shown in the background.

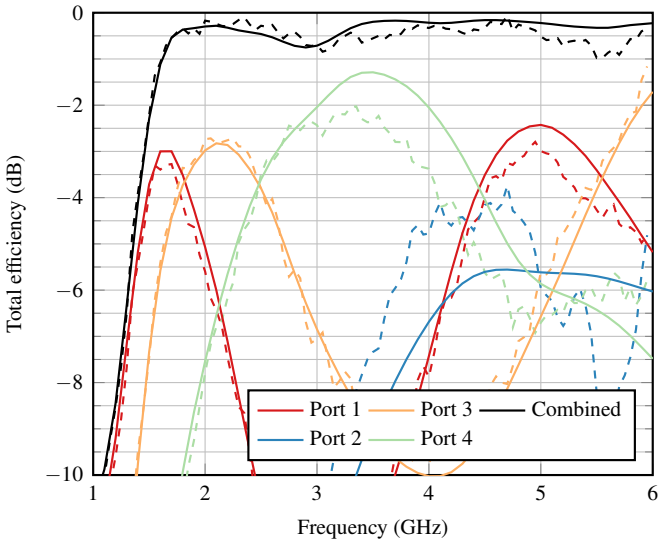

Fig. 8. Measured (dashed lines) and simulated (solid lines) total efficiencies of the four antenna ports, and the total efficiency obtained from the weighted superposition of all the four antennas.

parameters and the efficiencies of each port. We also calculate TARC for the entire system based on the scattering matrix using (3). These results are shown in Fig. 7. The resonances are shifted to lower frequencies, especially those of the shortest antenna elements. Nevertheless, the TARC performance is quite similar.

The far-field properties and the efficiency of the antenna are measured using the SATIMO Stargate 64 measurement system. We can only measure up to 6 GHz due to the limitations of the measurement system. The single-port efficiencies are directly calculated by the measurement system, after calibrating it with a reference horn antenna. These efficiencies are shown in Fig. 8. The results agree mostly with the simulations, with the differences being expected from the scattering parameter measurements shown in Fig. 7.

The efficiency of the simultaneous excitation can be estimated from the weighted sum of the individually measured fields. We obtain the efficiency by measuring the radiation intensity $U(\theta,\phi)$ at each measurement angle [28]

$$U(\theta,\phi) = B_0\left(|E_\theta(\theta,\phi)|^2 + |E_\phi(\theta,\phi)|^2\right) \tag{8}$$

where B_0 is a constant obtained from the calibration of the measurement system and E_θ and E_ϕ are the θ and ϕ components of the electric fields. These can then be summed to obtain the total radiated power P_{rad}. The total efficiency η_{tot} is found by comparing the radiated power to the available power P_{avail}

$$\begin{aligned}\eta_{\text{tot}} &= \frac{P_{\text{rad}}}{P_{\text{avail}}} \\ &= B_0 \int_0^{2\pi}\int_0^{\pi} \left(|E_\theta(\theta,\phi)|^2 + |E_\phi(\theta,\phi)|^2\right)\sin\theta d\theta d\phi\end{aligned} \tag{9}$$

where the available power P_{avail} has been included in the B_0 via the calibration.

The weights for calculating the efficiency of the simultaneous excitation are obtained from the scattering parameters. We sum both components of the electric fields of each antenna element after weighting them with the weighting coefficient a_i

$$E_\theta(\theta,\phi) = \sum a_i E_{\theta i}(\theta,\phi) \tag{10}$$

$$E_\phi(\theta,\phi) = \sum a_i E_{\phi i}(\theta,\phi) \tag{11}$$

The resulting field is then used to calculate the efficiency from (9). To ensure the efficiency calculation is still valid, the weights are normalized in a way to keep the input power the same as in the single-excitation case, i.e.

$$\sum |a_i|^2 = 1. \tag{12}$$

This calculation is also performed for the simulated electric fields. The results are shown in Fig. 8. The measured efficiencies agree well with the simulated efficiencies. The result shows that the efficiency obtained with the properly weighted multiport excitation is higher than the efficiency in any of the single-excitation cases.

Because the individual antenna elements do not have identical radiation patterns, weighting them modifies the resulting radiation pattern somewhat. To illustrate this effect, Fig. 9 shows the E-field patterns in the azimuth plane of the prototype. The patterns are shown for 2 and 4.3 GHz, with both simulated and measured results. The port numbering follows the same color scheme as in earlier figures, with the black curves representing the weighted superposition of the individual antenna patterns. The superposition is obtained from (10), (11) with the condition specified in (12). The results show that the radiation pattern is not significantly altered. The combined pattern is also stronger in all cases, as expected due to the increase in efficiency depicted in Fig. 8. Similar results can be obtained for other planes. Note that the pattern of the second antenna port is not shown at 2 GHz because it is an order of magnitude lower than the other ports, and does not meaningfully contribute to the result at 2 GHz.

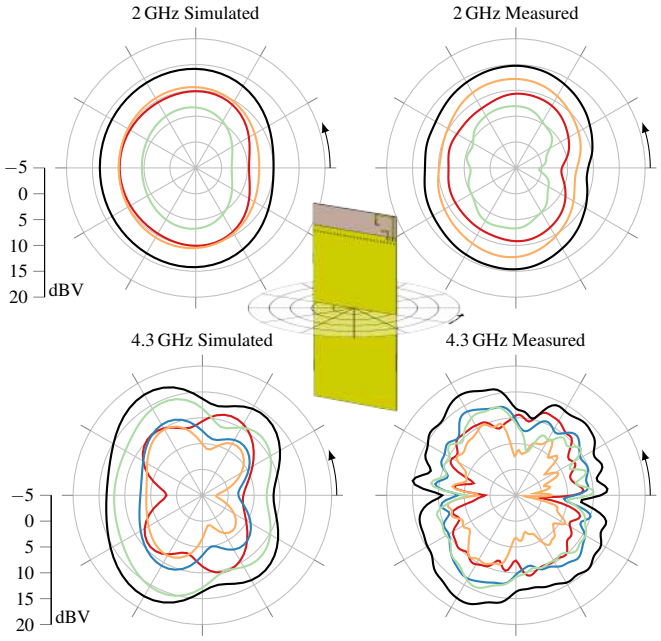

Fig. 9. The total E-field patterns for the simultaneous excitation (black curve) and for the individual elements.

TABLE I
THE OPTIMAL EXCITATION COEFFICIENTS FOR THE FOUR ANTENNA ELEMENTS AT 2 AND 4.3 GHZ.

	2 GHz	4.3 GHz
1	$-4.56\,\text{dB}\angle 161.7°$	$-7.1\,\text{dB}\angle -118.1°$
2	$-21.9\,\text{dB}\angle -17.6°$	$-7.1\,\text{dB}\angle -72.6°$
3	$-3.33\,\text{dB}\angle 90.2°$	$-10.6\,\text{dB}\angle 82.6°$
4	$-7.57\,\text{dB}\angle 0°$	$-2.8\,\text{dB}\angle 0°$

B. Simultaneous Excitation

So far, we have estimated the performance of our antenna concept mathematically. However, to demonstrate actual operation of our concept, we would need to feed all the antennas simultaneously.While the final implementation of our concept would use variable-gain power amplifiers and phase shifting implemented on the transceiver chip itself, there is no such chip available at this time. The concept presented here will require dedicated integrated circuit design to implement. As a proof-of-concept, and to encourage the research of the IC, we manufactured two power divider networks. These networks are used to generate the correct weights at a specific frequency. Although they operate at a fixed frequency, they nevertheless show how the antenna can be made to operate at different frequencies. The limitations of the integrated circuits will differ from those of the power divider networks, and as such, the results presented in this paper can only be used to evaluate the antenna performance. Further research is needed to quantify the overall performance of the system.

Table I lists the optimal weight coefficients at two different frequencies, obtained from the results depicted in Fig. 6. Two designs were made, one for 2 GHz and another for 4.3 GHz. The individual port reflection coefficients for these two cases, calculated from (2), are shown in Fig. 10. By comparing to Fig. 7 it can be seen that at the optimization frequency

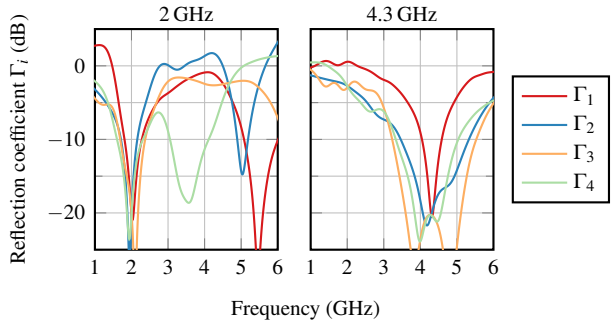

Fig. 10. Simulated active reflection coefficients for the two excitations specified in Table I.

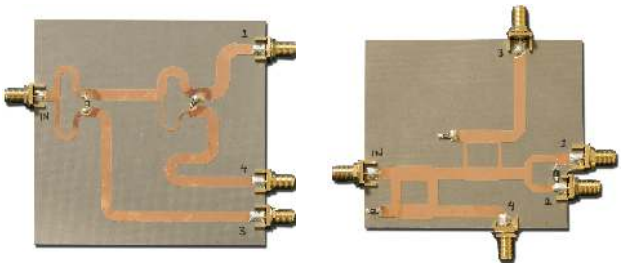

(a) (b)

Fig. 11. The power dividers manufactured to generate correct excitations at (a) 2 GHz and (b) 4.3 GHz.

the individual port reflections all equal the TARC. It should be noted that because the reflection coefficient also includes power fed from the other ports, it can be larger than one. This occurs when the power coupled from the other ports is larger than the power fed to the port. However, it should be noted that a large reflection coefficient does not necessarily result in high reflected power. If the input signal a_i is small, then the absolute power reflected will also be small despite the large reflection coefficient.

The frequencies were chosen based on the feasibility of the microstrip implementation. Fig. 11 illustrates the final feed network prototypes. The multiport power dividers were designed by combining multiple dividers together. Wilkinson power dividers were used when possible and hybrid couplers were used to obtain power division ratios that were not realizable using Wilkinson dividers.

These components are theoretically lossless (when acting as dividers), so they enable us to obtain a high total efficiency for the antenna and the feed network. The phase shifts are obtained by varying the microstrip line lengths in the designs. The 2 GHz design lacks the second antenna port, because at that frequency the power fed to that antenna element is insignificantly small. The second antenna element is instead terminated with a matched 50 Ω load.

Because the power dividers are lossy in the reverse direction, measuring the reflection coefficient from the input port is not relevant. To obtain relevant results, we must measure the efficiency from the far field. We measured the antenna with the simultaneous excitation using the same measurement setup as with the single-port measurements. Fig. 12 depicts the

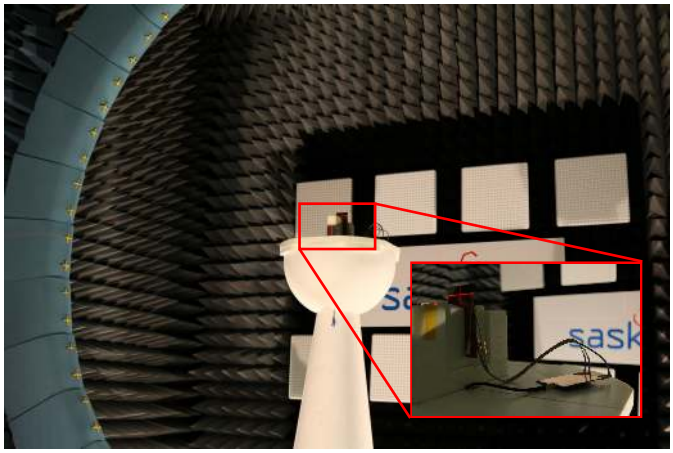

Fig. 12. Radiation pattern and total efficiency measurement using a SATIMO Stargate 64.

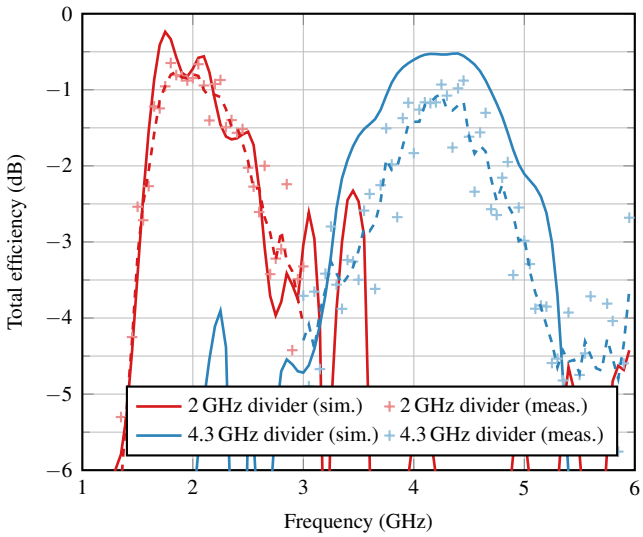

Fig. 13. Simulated and measured total efficiency for the antenna when fed with the 2 and 4.3 GHz dividers. The dashed curves represent the three-point moving average of the measurement data.

measurement setup. Due to the difficulties in the feed cable placement, the feed network had to be placed between the antenna and some of the probes of the Stargate.

Fig. 13(a) shows that we can obtain an efficiency of −0.85 dB with the 2 GHz divider and with the other divider we obtain an efficiency of −0.93 dB at 4.3 GHz, as illustrated by Fig. 13. Simulated results are shown for comparison. The simulation result is obtained by combining the simulated scattering parameters of the antenna and feed network in the circuit simulator of CST Design Studio. The expected antenna efficiency based on the results depicted in Fig. 8 would have been −0.4 dB and −1.5 dB at 2 and 4.3 GHz, respectively. However, the measured dividers have an insertion loss of 0.5 and 0.6 dB at the respective operating frequencies. The discrepancy between the measured and simulated results is explained by the manufactured 4.3 GHz divider having roughly 0.4 dB additional loss at the operating frequency when compared to the simulation result. Nevertheless, the results illustrate how the antenna changes the operation frequency based on the feed weighting.

The results presented here assume that the transceiver can feed the antennas optimally without a loss in performance. However, that is not the case in practice. For example, it is well known that the drawing less than maximal amplitude from a power amplifier will reduce its efficiency [26]. Nevertheless, the highly efficient antenna performance suggests that it is feasible to go forward with the transceiver design. Further research must be conducted to realize the concept and to produce quantitative results on the overall performance of the system.

V. Conclusion

In this paper we obtained several important results. We proved the operation of the cluster antenna by measurement and we demonstrated that a mobile form factor is possible. We showed additional measurement results for the frequency reconfigurable antenna. The reported efficiency is directly measured from the power radiated to the far field and the power fed to the input port of the feed network. Therefore there are no theoretical hypotheses or assumptions in these results, thus showing that the antenna can indeed be made to operate efficiently at different frequencies by weighting the input signals to the antenna.

From the antenna point of view, the concept functions well. The antenna design presented here is still rather preliminary, so there likely is still room for optimization. Each antenna element adds size and complexity to the transceiver, therefore being able to realize the concept with fewer antenna elements would be preferable. It is also quite relevant to investigate how efficiently the concept can be realized in the low band, i.e. below 1 GHz, where the tuning would be even more favorable.

Our power dividers were fixed to a specific frequency and were rather large structures. As such, they were only used to prove the concept. The next task is to fully realize the concept, i.e. to design the integrated circuit transceiver. So far it has become apparent that the nonidealities of the transceiver reduce the effectiveness of this approach. The weighting coefficients needed to obtain an optimally efficient antenna might not be efficient from the transceiver point of view. Therefore we need to investigate further how the antenna and the transceiver operate together.

Acknowledgments

The authors would like to thank Dr. M. Keskilammi from Sasken Finland for providing the measurement facilities for the far-field measurements.

References

[1] "5G: a technology vision," White Paper, Huawei Technologies, 2013.
[2] "Looking ahead to 5G," White Paper, Nokia Networks, 2015.
[3] J. Andrews, S. Buzzi, W. Choi, S. Hanly, A. Lozano, A. Soong, and J. Zhang, "What will 5G be?" *IEEE J. Sel. Areas Commun.*, vol. 32, no. 6, pp. 1065–1082, Jun. 2014.
[4] L. J. Chu, "Physical limitations of omni-directional antennas," *J. Appl. Phys.*, vol. 19, no. 12, pp. 1163–1175, Dec. 1948.

[5] R. F. Harrington, "Effect of antenna size on gain, bandwidth, and efficiency," *J. Res. Nat. Bur. Stand*, vol. 64, no. 1, pp. 1–12, Jan.–Feb. 1960.
[6] H. Wheeler, "Small antennas," *IEEE Trans. Antennas Propag.*, vol. 23, no. 4, pp. 462–469, Jul. 1975.
[7] J. Ilvonen, R. Valkonen, J. Holopainen, and V. Viikari, "Multiband frequency reconfigurable 4G handset antenna with MIMO capability," *Prog. Electromagn. Res.*, vol. 148, pp. 233–243, 2014.
[8] S. Caporal Del Barrio, A. Tatomirescu, G. Pedersen, and A. Morris, "Novel architecture for LTE world-phones," *IEEE Antennas Wireless Propag. Lett.*, vol. 12, pp. 1676–1679, 2013.
[9] R. Valkonen, C. Luxey, J. Holopainen, C. Icheln, and P. Vainikainen, "Frequency-reconfigurable mobile terminal antenna with MEMS switches," in *Proc. 4th Eur. Conf. Antennas Propag. (EuCAP)*, Barcelona, Spain, Apr. 2010, pp. 1–5.
[10] R. Valkonen, M. Kaltiokallio, and C. Icheln, "Capacitive coupling element antennas for multi-standard mobile handsets," *IEEE Trans. Antennas Propag.*, vol. 61, no. 5, pp. 2783–2791, May 2013.
[11] Y. Li, Z. Zhang, J. Zheng, Z. Feng, and M. Iskander, "A compact hepta-band loop-inverted F reconfigurable antenna for mobile phone," *IEEE Trans. Antennas Propag.*, vol. 60, no. 1, pp. 389–392, Jan. 2012.
[12] D. Rodrigo, B. A. Cetiner, and L. Jofre, "Frequency, radiation pattern and polarization reconfigurable antenna using a parasitic pixel layer," *IEEE Trans. Antennas Propag.*, vol. 62, no. 6, pp. 3422–3427, Jun. 2014.
[13] X.-l. Yang, J.-c. Lin, G. Chen, and F.-l. Kong, "Frequency reconfigurable antenna for wireless communications using GaAs FET switch," *IEEE Antennas Wireless Propag. Lett.*, vol. 14, pp. 807–810, 2015.
[14] J.-M. Hannula, J. Holopainen, and V. Viikari, "Concept for frequency reconfigurable antenna based on distributed transceivers," *IEEE Antennas Wireless Propag. Lett.*, vol. 16, pp. 764–767, 2017.
[15] O. Alrabadi, A. Tatomirescu, M. Knudsen, G. Pedersen, M. Pelosi, S. Caporal Del Barrio, P. Olesen, and P. Bundgaard, "Antenna tuning via multi-feed transceiver architecture," U.S. Patent Application 20 140 062 813, Mar. 6, 2014.
[16] C. Volmer, J. Weber, R. Stephan, K. Blau, and M. Hein, "An eigen-analysis of compact antenna arrays and its application to port decoupling," *IEEE Trans. Antennas Propag.*, vol. 56, no. 2, pp. 360–370, Feb. 2008.
[17] C. Volmer, M. Sengul, J. Weber, R. Stephan, and M. Hein, "Broadband decoupling and matching of a superdirective two-port antenna array," *IEEE Antennas Wireless Propag. Lett.*, vol. 7, pp. 613–616, 2008.
[18] C. Volmer, J. Weber, R. Stephan, and M. Hein, "A descriptive model for analyzing the diversity performance of compact antenna arrays," *IEEE Trans. Antennas Propag.*, vol. 57, no. 2, pp. 395–405, Feb. 2009.
[19] "World radiocommunication conference allocates spectrum for future innovation," Press Release, Nov. 2015. [Online]. Available: http://www.itu.int/net/pressoffice/press_releases/2015/56.aspx#.WKVnfk7y2jA
[20] A. A. Al-Hadi, J. Ilvonen, R. Valkonen, and V. Viikari, "Eight-element antenna array for diversity and MIMO mobile terminal in LTE 3500 MHz band," *Microw. Opt. Technol. Lett.*, vol. 56, no. 6, pp. 1323–1327, 2014.
[21] K.-L. Wong and J.-Y. Lu, "3.6-GHz 10-antenna array for MIMO operation in the smartphone," *Microw. Opt. Technol. Lett.*, vol. 57, no. 7, pp. 1699–1704, 2015.
[22] M. Y. Li, Y. L. Ban, Z. Q. Xu, G. Wu, C. Y. D. Sim, K. Kang, and Z. F. Yu, "Eight-port orthogonally dual-polarized antenna array for 5G smartphone applications," *IEEE Trans. Antennas Propag.*, vol. 64, no. 9, pp. 3820–3830, Sep. 2016.
[23] Y. L. Ban, C. Li, C. Y. D. Sim, G. Wu, and K. L. Wong, "4G/5G multiple antennas for future multi-mode smartphone applications," *IEEE Access*, vol. 4, pp. 2981–2988, 2016.
[24] M. Manteghi and Y. Rahmat-Samii, "Multiport characteristics of a wide-band cavity backed annular patch antenna for multipolarization operations," *IEEE Trans. Antennas Propag.*, vol. 53, no. 1, pp. 466–474, Jan. 2005.
[25] J.-M. Hannula, J. Holopainen, and V. Viikari, "Further investigations on the behavior of a frequency reconfigurable antenna cluster," in *Proc. 11th Eur. Conf. Antennas Propag. (EuCAP)*, Paris, France, 2017.
[26] T. Johansson and J. Fritzin, "A review of watt-level CMOS RF power amplifiers," *IEEE Trans. Microw. Theory Tech.*, vol. 62, no. 1, pp. 111–124, Jan. 2014.
[27] Y. Fu and G.-M. Yang, "Design of compact multiband MIMO antenna for the mobile handsets," *Microw. Opt. Technol. Lett.*, vol. 58, no. 10, pp. 2411–2415, Oct. 2016.
[28] C. A. Balanis, *Antenna theory: analysis and design*, 3rd ed. Hoboken, NJ: John Wiley & Sons, 2005.

Jari-Matti Hannula (S'16) was born in Luvia, Finland, in 1990. He received the B.Sc. (Tech.) and M.Sc. (Tech.) degrees (with distinction) in electrical engineering from Aalto University, Espoo, Finland, in 2014 and 2015, and is currently pursuing the D.Sc. (Tech.) degree at the same university.

He has been with the Department of Electronics and Nanoengineering, Aalto University School of Electrical Engineering since 2013, first as a Research Assistant and since 2015 as a Doctoral Candidate. His current research interests include electrically small antennas and techniques for improving and analyzing their performance.

Tapio Saarinen was born in Helsinki, Finland, in 1994. He received the Bachelor of Science (Tech.) degree in electrical engineering from Aalto University School of Electrical Engineering, Espoo, Finland, in 2017, and is currently working toward the Master of Science (Tech.) degree in electrical engineering at the same university.

He has worked as a Teaching Assistant on courses related to circuit theory and power engineering at Aalto University since 2015. In summer 2016 and since the beginning of 2017, he has worked as a Research Assistant at the Department of Electronics and Nanoengineering, Aalto University.

Jari Holopainen received the M.Sc. degree in 2005 from Helsinki University of Technology, Espoo, Finland, the D.Sc. degree in electrical engineering in 2011 from Aalto University, and the professional teacher education in 2015 from Häme University of Applied Sciences, Hämeenlinna, Finland.

Currently, he is a University Lecturer in the Department of Electronics and Nanoengineering, Aalto University School of Electrical Engineering. His current scientific interests include university pedagogy, microwave engineering, and antennas.

Ville Viikari (S'06–A'09–M'09–SM'10) was born in Espoo, Finland, in 1979. He received the Master of Science (Tech.) and Doctor of Science (Tech.) (with distinction) degrees in electrical engineering from the Helsinki University of Technology (TKK), Espoo, Finland, in 2004 and 2007, respectively.

He is currently an Associate Professor and Deputy Head of Department with the Aalto University School of Electrical Engineering, Espoo, Finland. From 2001 to 2007, he was with the Radio Laboratory, TKK, where he studied antenna measurement techniques at submillimeter wavelengths and antenna pattern correction techniques. From 2007 to 2012, he was a Research Scientist and a Senior Scientist with the VTT Technical Research Centre, Espoo, Finland, where his research included wireless sensors, RFID, radar applications, MEMS, and microwave sensors. His current research interests include antennas for mobile networks, RF-powered devices, and antenna measurement techniques.

Dr. Viikari has served as the chair of the Technical Program Committee of the ESA Workshop on Millimetre-Wave Technology and Applications and the Global Symposium on Millimeter Waves (GSMM) twice, in 2011 and 2016 in Espoo, Finland. He was the recipient of the Young Researcher Award of the Year 2014, presented by the Finnish Foundation for Technology Promotion, IEEE Sensors Council 2010 Early Career Gold Award, the 2008 Young Scientist Award of the URSI XXXI Finnish Convention on Radio Science, Espoo, Finland, and the Best Student Paper Award of the annual symposium of the Antenna Measurement Techniques Association, Newport, RI, USA (October 30November 4, 2005).